JACS
JOURNAL OF THE AMERICAN CHEMICAL SOCIETY
Article
pubs.acs.org/JACS

Computational Design of Non-natural Sugar Alcohols to Increase Thermal Storage Density: Beyond Existing Organic Phase Change Materials

Taichi Inagaki*,†,‡,# and Toyokazu Ishida*,†,‡

†Research Center for Computational Design of Advanced Functional Materials (CD-FMat), National Institute of Advanced Industrial Science and Technology (AIST), Tsukuba Central 2, 1-1-1 Umezono, Tsukuba, Ibaraki 305-8568, Japan

‡Thermal Management Materials and Technology Research Association (TherMAT), 1-5-11, Nishishinbashi, Minato-ku, Tokyo 105-0003, Japan

Supporting Information

ABSTRACT: Thermal storage, a technology that enables us to control thermal energy, makes it possible to reuse a huge amount of waste heat, and materials with the ability to treat larger thermal energy are in high demand for energy-saving societies. Sugar alcohols are now one promising candidate for phase change materials (PCMs) because of their large thermal storage density. In this study, we computationally design experimentally unknown non-natural sugar alcohols and predict their thermal storage density as a basic step toward the development of new high performance PCMs. The non-natural sugar alcohol molecules are constructed in silico in accordance with the previously suggested molecular design guidelines: linear elongation of a carbon backbone, separated distribution of OH groups, and even numbers of carbon atoms. Their crystal structures are then predicted using the random search method and first-principles calculations. Our molecular simulation results clearly demonstrate that the non-natural sugar alcohols have potential ability to have thermal storage density up to ∼450−500 kJ/kg, which is significantly larger than the maximum thermal storage density of the present known organic PCMs (∼350 kJ/kg). This computational study suggests that, even in the case of H-bonded molecular crystals where the electrostatic energy contributes mainly to thermal storage density, the molecular distortion and van der Waals energies are also important factors to increase thermal storage density. In addition, the comparison between the three eight-carbon non-natural sugar alcohol isomers indicates that the selection of preferable isomers is also essential for large thermal storage density.

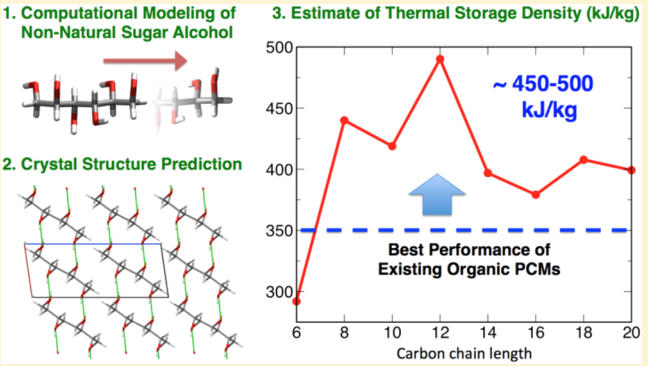

1. INTRODUCTION

Reusing a huge amount of waste heat exhausted from our daily lives and industry is one of the most important issues for energy-saving societies. Thermal storage, a technology that enables us to control thermal energy, has recently attracted much attention because the technology makes it possible to effectively reuse such heat.[1,2] Substances utilized in the technology, i.e., thermal storage materials, are generally classified into sensible heat, latent heat, and chemical heat storage materials.[3] In terms of the balance between the handling of large amounts of heat and practical utility, latent heat storage materials that store/release thermal energy by taking advantage of phase transitions are supposed to be particularly useful. Because of the feature of the latent heat storage manner, those materials are also known as phase change materials (PCMs).[4−6]

High performance PCMs are crucially important for the effective reuse of waste heat. The most significant thermophysical property to measure the performance is latent heat per unit mass, which is generally called *thermal storage density*. Recently, novel inorganic PCMs utilizing a solid−solid phase transition, such as Ti_3O_5 and VO_2, have been developed.[7] These materials have many characteristic properties other than thermal storage, so that they are expected to be utilized as useful functional materials. However, they store a tiny amount of thermal energy, for example Ti_3O_5 has thermal storage density of ∼50 kJ/kg,[7] which is much smaller than water (330 kJ/kg[8]). Unlike these inorganic PCMs, typical organic PCMs include *n*-paraffin series.[9] They are categorized into the solid−liquid phase transition type of PCMs which store and release thermal energy by melting and crystallization, respectively, and are partly utilized in practice. Organic *n*-paraffins also have smaller thermal storage density than water, but they are able to treat a medium amount of thermal energy (∼240 kJ/kg) depending on their carbon chain lengths. Beyond the *n*-paraffin series, sugar

Received: June 8, 2016
Published: August 9, 2016

DOI: 10.1021/jacs.6b05902
J. Am. Chem. Soc. 2016, 138, 11810−11819

alcohol series are widely known as organic PCMs, which have thermal storage density comparable to that of water.[10,11]

Sugar alcohols are polyalcohols generated by reducing carbohydrates. They have received much attention in food and pharmaceutical industries[12,13] due to their various unique properties which stem from intermolecular and intramolecular hydrogen bonds (H-bonds) formed by a number of hydroxyl (OH) groups. In recent years, investigations that treat sugar alcohols as PCMs have become more active in order to exploit their large thermal storage density. For example erythritol, one of the four-carbon sugar alcohols, has the largest class of thermal storage density (~340 kJ/kg) in existing organic PCMs,[6] so that a number of studies have been performed to solve practical problems such as supercooling phenomena and low thermal diffusivity coefficients.[14,15] However, even in sugar alcohols, an amount of stored thermal energy has an upper bound of ~350 kJ/kg under the present known organic materials.[6] (The best performance of ~350 kJ/kg is obtained from galactitol, one of the six-carbon sugar alcohols.) It has been unclear how large thermal storage density can be achieved potentially in the case of organic PCMs. The question is very critical, but it has hardly been investigated, neither experimentally nor computationally, as long as we know. If we can drastically improve the potential ability of PCMs, the thermal storage technology will become more promising tool for handling waste heat and will be more broadly applied to the modern society. This is the final goal of our research.

As a basic step toward the final goal, we first focused on sugar alcohols, one of the promising organic PCMs. Similar to *n*-paraffin series, sugar alcohols with different carbon chain lengths (from four to eight carbon atoms) occur naturally. In addition, even with the same carbon chain length, there are some stereoisomers with different OH group locations. These two features of sugar alcohols may affect their thermal storage density. What kind of sugar alcohols are most suitable for handling a large amount of thermal energy? In order to answer the question, we more recently focused on six-carbon natural sugar alcohols and revealed the molecular mechanism of their thermal storage and the origin of the difference of thermal storage density between four stereoisomers using a molecular dynamics (MD) simulation technique.[16] According to the results, we proposed three molecular design guidelines in order to construct new sugar-alcohol-like PCMs with large thermal storage density (more than 350 kJ/kg). The proposed guidelines were (1) linear elongation of a carbon backbone, (2) separated distribution of OH groups, and (3) even numbers of carbon atoms in a carbon backbone. It was shown in that study that in the case of sugar alcohols a majority of the released/stored thermal energy originates from the change of electrostatic (ES) interaction energy associated with formation/disruption of intermolecular H-bonds in the solid−liquid phase transition. Thus, we expected that the guideline (1) increases OH groups, which would result in a further large change of ES interaction energy due to the increasing difference of the number of intermolecular H-bonds between the solid and liquid phases. In addition, it was also shown that some six-carbon sugar alcohol isomers are destabilized in the crystal by intramolecular ES repulsion between two close oxygen atoms. The solid phase with thus destabilized sugar alcohol molecules was illustrated to result in significantly small thermal storage density. On the basis of the fact, we also expected that the guideline (2) would lead to isomers which form the energetically stable solid phase. The guideline (3) was derived from the additional statistical survey. Although these propositions, particularly guidelines (1) and (2), were certainly suggested on the basis of the simulation results of six-carbon sugar alcohols, they have not been justified yet whether thus designed molecules actually have much larger thermal storage density compared to the existing natural sugar alcohols. Therefore, the main purpose of this study is to demonstrate how large amounts of thermal energy can be stored in the molecules designed as an extension of natural sugar alcohols.

Another interest in this study is a computational strategy for developing new PCMs. Computational approaches have become more and more inevitable in the field of material science.[17,18] They enable us to obtain a number of relatively high-quality information on materials at the atomic scale. Comparing to trial-and-error approaches, material searches based on computationally rational strategy are expected to significantly reduce cost and time involved with developing new materials. However, in the area of thermal storage materials, in particular PCMs, there are very few such studies using computational approaches, as long as we know. Therefore, computational thermophysical property predictions for various materials including experimentally unknown ones are in high demand for the effective development of new PCMs in a short period of time at low cost.

In this paper, we construct new sugar-alcohol-like molecules in silico according to above three molecular design guidelines and predict their thermal storage densities by MD simulations. As mentioned above, PCMs based on solid−liquid phase transition store heat by melting and release by crystallization, but it is quite difficult to simulate crystallizations of such complex molecules. Thus, we focus only on the melting (i.e., heat storage) process in this paper. New molecules presented here are seven acyclic polyalcohols. They have a linear saturated carbon chain with even numbers of carbon atoms from 8 through 20 and have an OH group on each carbon atom (Figure 1). Straight-chain polyalcohols with more than six

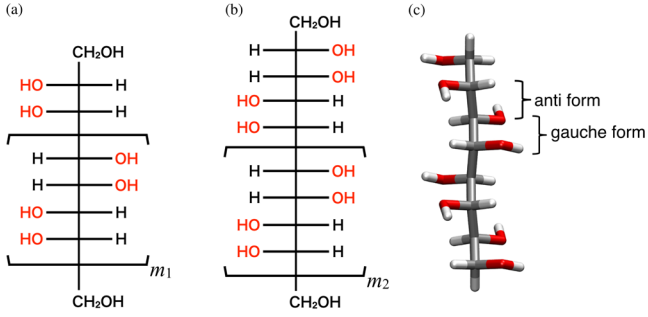

Figure 1. Chemical formulas of non-natural sugar alcohols with even numbers of carbon atoms from 8 through 20: (a) **C8**, **C12**, **C16**, and **C20** sugar alcohols are, respectively, obtained by m_1 = 1, 2, 3, and 4, and they are achiral compounds. (b) **C10**, **C14**, and **C18** sugar alcohols are, respectively, obtained by m_2 = 1, 2, and 3, and they are chiral compounds. (c) Molecular structure of the **C8** sugar alcohol in the extended conformation as an example. Mannitol, one of the six-carbon natural sugar alcohols, is obtained by m_2 = 0.

carbon atoms $C_nH_{n+2}(OH)_n$ ($n > 6$) are rarely found in nature. Indeed, the designed new molecules have never been reported in nature at present. For this reason, in this paper, we call these molecules collectively non-natural sugar alcohols and call each molecule **Cn** sugar alcohol using the number of carbon atoms *n*. As expected, crystal structures of these non-natural sugar

DOI: 10.1021/jacs.6b05902
J. Am. Chem. Soc. 2016, 138, 11810−11819

alcohols have not been obtained experimentally. Therefore, we predict their crystal structures using computational chemistry methods. With the predicted crystal structures we then estimate their melting points and thermal storage densities. We examine how these thermal storage densities were attained from the two guidelines (1) and (2), i.e., the effect of the guidelines on thermal storage density. Finally, we clearly demonstrate that the non-natural sugar alcohols have potential ability to have thermal storage density up to 450−500 kJ/kg, which is significantly larger than the maximum thermal storage density of the present known organic PCMs.

2. COMPUTATIONAL METHODS

For predicting thermal storage density of non-natural sugar alcohols, a set of calculations outlined below were performed in the following order. Practical details are given in Supporting Information.

(i) **Molecular modeling.** Non-natural sugar alcohols were constructed according to the molecular design guidelines.

(ii) **Crystal structure prediction: Trial crystal structure generation.** A huge number of trial crystal structures were generated by the Monte Carlo like random search method.[19] In this step, geometry optimizations, energy calculations, and provisional ranking of trial crystal structures were performed with a molecular force field. This step guarantees that the crystal structure prediction in this study was performed without any help from experiments. Calculations in this step were performed using the UPACK program package.[19]

(iii) **Crystal structure prediction: Ranking.** The candidates selected from the trial crystal structures were ranked according to the higher-accuracy first-principles calculations. The most energetically stable crystal structure in this step was finally adopted as the most likely crystal structure. First-principles calculations were performed using the Quantum Espresso program package.[20]

(iv) **Thermophysical property calculation: Melting point.** Before estimating thermal storage density, we need to predict a melting point. In this study, melting points were predicted by the interface/*NPT* method, where independent *NPT* simulations with different temperatures were performed via a solid−liquid two-phase configuration.[16,21] This method is preferable to the present purpose to predict a melting point trend of non-natural sugar alcohols on a semiquantitative level because it enables to avoid some overestimates of melting points at an affordable computational cost by introducing solid−liquid heterogeneous interfaces.

(v) **Thermophysical property calculation: Thermal storage density.** Since thermal storage density is defined as the enthalpy of fusion per unit mass, it was estimated from solid-phase and liquid-phase enthalpies calculated by *NPT* simulations at the predetermined melting point. All MD simulations including melting point calculations were performed with the AMBER force field[22] combined with the OPLS charge set.[23] This hybrid force field has been shown, in our previous study,[16] to be reasonable to describe melting points and thermal storage densities of sugar alcohols. These MD simulations were carried out with the Gromacs program package.[24]

Many studies have validated this two-step crystal structure prediction method,[25,26] but in order to obtain further confirmation we applied the procedure to mannitol. Mannitol is one of the six-carbon natural sugar alcohols whose crystal structure is experimentally known. The result showed that the predicted crystal structure was quite identical to the experimental one (D-mannitol), which indicates that the crystal structure prediction was successfully accomplished. Therefore, we expect that this prediction method also works well for non-natural sugar alcohols.

3. RESULTS

3.1. Non-natural Sugar Alcohol Molecules. In accordance with the molecular design guidelines mentioned in Introduction, we first constructed new molecules as an extension of natural sugar alcohols, i.e., non-natural sugar alcohols (Figure 1). To our knowledge, these molecules have never been found in nature and have also never been artificially synthesized by chemical methods so far. A linear and long carbon chain with the same number of OH groups as carbon atoms satisfies the guideline (1), i.e., the linear elongation of a carbon backbone. The guideline (2) that OH groups should be distributed separately as far as possible is accomplished by the two structural features: absence of 1−3 parallel interactions in the extended conformation and structurally possible anti conformations of vicinal OH groups. It should be noted that the 1−3 parallel interaction is repulsive interaction between a C−O bond and a second neighboring C−O bond with a parallel bond direction to the former and is known to cause large electrostatic instability in sugar alcohol molecules because of a remarkably short distance between the two oxygen atoms (∼2.5 Å).[27] Concretely speaking, CHOH−CHOH units with an anti conformation of OH groups are connected to each other as newly neighboring OH groups take a gauche conformation (Figure 1c). Furthermore, molecules with even carbon atoms from 8 through 20 are constructed following the guideline (3). These molecules can be regarded as the extension of a mannitol molecule which is obtained by m_2 = 0 in Figure 1b.[28] It should be noted that the **C8**, **C12**, **C16**, and **C20** sugar alcohols depicted in Figure 1a are achiral (meso) compounds whereas the **C10**, **C14**, and **C18** sugar alcohols depicted in Figure 1b are chiral compounds. Thus, the formers have a slightly higher-symmetry structure than the latters.

3.2. Crystal Structures of the Non-natural Sugar Alcohols. Next we predicted crystal structures of the non-natural sugar alcohols constructed above. The detailed processes and results of the crystal structure predictions are summarized in Supporting Information. The predicted crystal structure of the **C8** sugar alcohol is displayed in Figure 2 as a representative example. We found that the predicted **C8** sugar alcohol's crystal structure is stabilized by its own intermolecular H-bond networks (green line in Figure 2) and, as expected, all OH groups are successfully incorporated in the networks. The motif of the H-bond networks was a ring type which is formed by four OH groups in four different molecules (Figure 2b). Such ring motif is familiar to water and ice structures,[29,30] and it is also observed in the experimental crystal structure of mannitol.[31]

Another important feature of this crystal structure is that there are no intermolecular H-bonds between end-group layers (Figure 2a). This is related to the molecular structure in the crystal that the OH groups bonded to the terminal carbon atoms are out of the plane formed by carbon atoms (Figure 2c). In that interlayer regions, instead of intermolecular H-bonds, weak noncovalent (such as dispersion or van der Waals) interactions mainly attract molecules to each other. Therefore, we found that this crystal structure is formed by the different kinds of cohesive forces depending on the direction. These two features are common characteristics of the predicted crystal structures of the **C8**−**C20** sugar alcohols.

3.3. Melting Points and Thermal Storage Densities. With the predicted crystal structures we estimated melting points and thermal storage densities of the **C8**−**C20** sugar

DOI: 10.1021/jacs.6b05902
J. Am. Chem. Soc. 2016, 138, 11810−11819

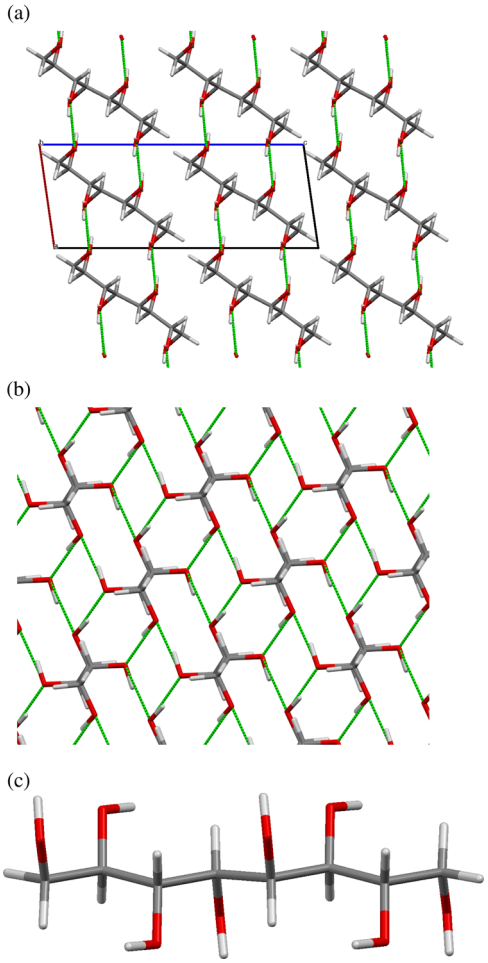

Figure 2. Crystal structure of the **C8** sugar alcohol obtained by the crystal structure prediction: (a) the view in the direction that carbon backbones can be seen like lines, (b) the view in the direction along a carbon backbone, and (c) molecular structure in the crystal. The green lines connecting oxygen atoms represent intermolecular H-bonds between the OH groups. The unit cell is shown in the panel (a).

alcohols by MD simulations. The results are displayed in Figure 3 and Table S4. In addition to these results, we also show the simulation results of mannitol (**C6** sugar alcohol) as a representative example of the six-carbon sugar alcohols with relatively large thermal storage density (290−308 kJ/kg[32]). For the qualitative comparison to the non-natural sugar alcohols, the melting point and thermal storage density of the **C6** sugar alcohol were calculated with the crystal structure predicted in the same manner as the non-natural sugar alcohols. The calculated melting point of the **C6** sugar alcohol was found to be 480 K, which is somewhat higher than the corresponding experimental value (~440 K[32]). Thus, we found that the present calculations may give small overestimates of melting points of the non-natural sugar alcohols. The predicted melting points of the **C8**−**C20** sugar alcohols (600−840 K) were much higher than that of the **C6** sugar alcohol (480 K). These melting points were found to increase with the carbon chain length except between the **C8** and **C10** sugar alcohols. This is because the increase in OH groups stemming from the carbon chain elongation enhances intermolecular attractive force per molecule through the increased intermolecular H-bonds. As a result, the solid phase becomes hard to melt in low temperatures as the carbon backbone becomes long.

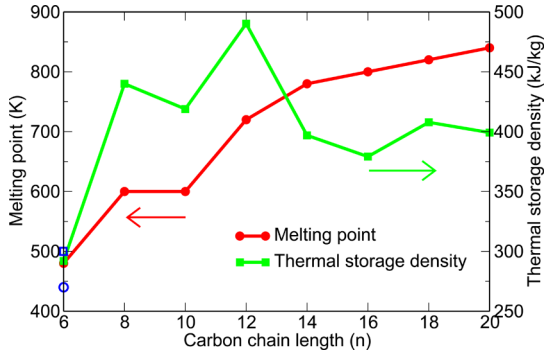

Figure 3. Melting points (K) and thermal storage densities (kJ/kg) of the **C6**−**C20** sugar alcohols obtained from MD simulations. Melting points (red color) and thermal storage densities (green color) are displayed on the left and right vertical axes, respectively. For the **C6** sugar alcohol (mannitol), the values obtained from the predicted crystal structure are shown. In addition, the experimental melting point and thermal storage density of mannitol are shown by an open blue circle and an open blue square, respectively.

As with the melting point, the thermal storage density of the **C6** sugar alcohol was calculated and found to be ~290 kJ/kg. This estimate is in good agreement with the corresponding experimental value (~300 kJ/kg[32]). The thermal storage densities of the **C8**−**C20** sugar alcohols (~375−500 kJ/kg) were much larger than that of the **C6** sugar alcohol (~290 kJ/kg). These remarkably large thermal storage densities indicate that the potential ability of the **C8**−**C20** sugar alcohols extends well beyond the existing organic PCMs in terms of thermal storage density. Unlike the melting points, however, the thermal storage densities were observed to have a unique trend: they do not necessarily increase with the carbon chain length. The largest thermal storage density is provided by the **C12** sugar alcohol (~500 kJ/kg) and the second largest is by the **C8** sugar alcohol (~450 kJ/kg). In addition, thermal storage densities of the **C14** sugar alcohol and the longer sugar alcohols greatly decrease compared to that of the **C12** sugar alcohol. As well as these apparent irregular patterns, the origin of the remarkably large thermal storage density of the non-natural sugar alcohols will be revealed in Section 3.5.

3.4. Premelting Phases of the C14−C20 Sugar Alcohols. In this section, we show *premelting phase* observed in the **C14**−**C20** sugar alcohols before analyses of thermal storage density. The premelting phase is important because it links to the relatively small thermal storage densities of the **C14**−**C20** sugar alcohols. Figure 4 shows enthalpy-temperature plots of the **C14**−**C20** sugar alcohols obtained from the interface/*NPT* simulations. The solid−liquid first-order phase transition is identified by an abrupt and large change in enthalpy, which can be seen at 780, 800, 820, and 840 K for the **C14**, **C16**, **C18**, and **C20** sugar alcohols, respectively. These temperatures are regarded as the melting points (see Figure 3). In addition to these changes, we can observe a small but obvious change in enthalpy at 680 K for the **C14** and **C18** sugar alcohols and at 740 K for the **C16** and **C20** sugar alcohols. This additional change in enthalpy indicates that a solid−solid phase transition occurs at that temperature. The solid phase at the high temperature side has larger enthalpy compared to that at the low temperature side. Thus, we found that the relatively small thermal storage densities of the **C14**−**C20** sugar alcohols originate from the enthalpy changes in the solid−solid phase transition. That is, the solid phase at the high temperature side

DOI: 10.1021/jacs.6b05902
J. Am. Chem. Soc. 2016, 138, 11810−11819

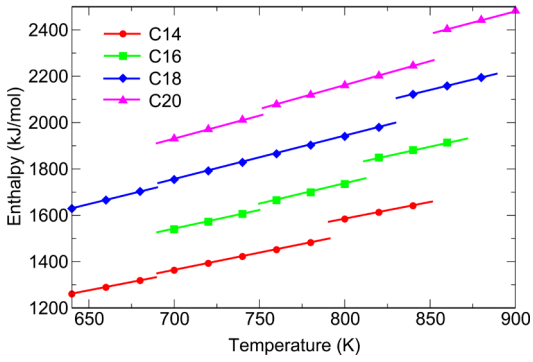

Figure 4. Plots of enthalpy per molecule (kJ/mol) along temperature (K) of the **C14**–**C20** sugar alcohols obtained from the interface/*NPT* simulations. The plots of the **C14**, **C16**, **C18**, and **C20** sugar alcohols are shown in red, green, blue, and magenta colors, respectively. The lines are drawn as the discontinuities of plots become clear.

already absorbs a part of fusion enthalpy (i.e., enthalpy difference between the perfect crystal and liquid phases) before melting. In fact, their whole thermal storage densities including the enthalpy change associated with the solid–solid phase transition are comparable to that of the **C12** sugar alcohol or slightly increase with the carbon chain length (Figure S3). This result suggests that the solid phase at the high temperature side transits partially to the liquid phase. For this reason, in this paper, we distinguish this solid phase as the premelting phase from the crystal phase at the low temperature side.

To characterize the premelting phases, we show representative configurations of the two solid phases of the **C14** sugar alcohol as an example. Figure 5a and b display, respectively, the configurations of the crystal phase at 680 K and the premelting phase at 700 K. Green dotted lines represent intermolecular H-bonds. In the view along the magenta arrows in Figure 5a, there are very few intermolecular H-bonds between end-group layers in the crystal phase and the ordered H-bond networks explained in Section 3.2 still remain. On the other hand, in the premelting phase, we can find that intermolecular H-bonds between end-group layers are newly formed and the H-bond networks in that region are dissolved (Figure 5b). This dissolution are related to the disordering of dihedral angles around C–C bonds in the terminal CH_2OH–CHOH segments (see Figure S4). Given that almost all of these dihedral angles in the crystal phase have a trans-type conformation, the 60–70% of these dihedral angles adopts a gauche-type conformation in the premelting phase, which is very similar to the percentage in the liquid phase. Therefore, the regions near end groups are heavily disordered by the solid–solid phase transition. The premelting phases of the **C16**–**C20** sugar alcohols are characterized in the same manner as the **C14** sugar alcohol by this disordering. Such disordering in end groups is well-known in *n*-paraffin series as "end-gauche defect".[33]

3.5. Analyses of Thermal Storage Densities: Effect of Carbon Chain Elongation. In Section 3.3, we found that the potential ability of the **C8**–**C20** sugar alcohols greatly exceeds existing organic PCMs in terms of thermal storage density. To clarify what interactions contribute to the remarkably large thermal storage densities and how the carbon chain elongation influences each contribution, we performed a decomposition analysis of thermal storage density. Thermal storage density is extremely well approximated by the potential energy difference between the solid and liquid phases at the melting point,[34] and

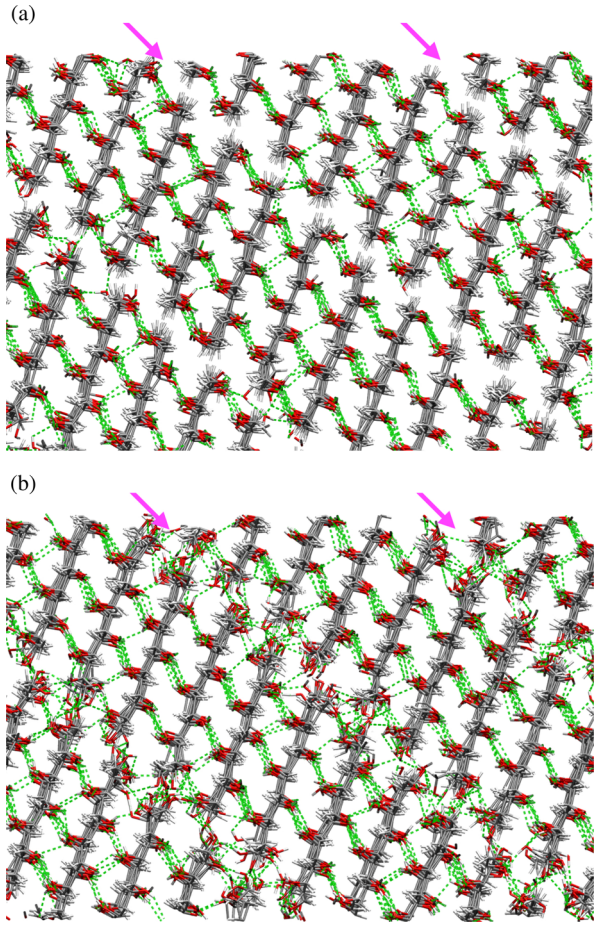

Figure 5. Representative solid phase configurations of the **C14** sugar alcohol at 680 K (a) and 700 K (b) obtained from the interface/*NPT* simulations. Green lines and magenta arrows represent intermolecular H-bonds and end-group layers, respectively.

potential energy is easily decomposed into several energy terms in the case of the classical force-field based simulation. In the present study, potential energies in each phase were decomposed into three energy terms: a bonded energy term including bond, angle, and dihedral angle (BAD) and two nonbonded energy terms, electrostatic (ES) and van der Waals (vdW) energies. The BAD energy comes from the distortion of molecular structures, and the vdW energy is somewhat related to molecular mass density (for example, packing density of crystals). In the case of sugar alcohol series, the ES energy originates mainly from interaction between OH groups, such as H-bonds. Since the thermal storage densities of the **C14**–**C20** sugar alcohols are affected by their premelting phases, it may not be appropriate to directly compare their decomposed energies with those of the **C6**–**C12** sugar alcohols. Thus, we first focus on the **C6**–**C12** sugar alcohols, and the **C14**–**C20** sugar alcohols are considered later.

Figure 6 and Table S5 compare the contributions of the BAD, ES, and vdW energies to the thermal storage densities of the **C6**–**C12** sugar alcohols. From the figure we found that the ES energy contributes largely to the thermal storage densities of the **C6**–**C12** sugar alcohols (~150–210 kJ/kg). This large contribution is attributed to the dissolution of intermolecular H-bond networks during the melting process. Following the leading ES energy, the BAD and vdW energies have the second and third largest contributions, respectively. These results are

DOI: 10.1021/jacs.6b05902
J. Am. Chem. Soc. 2016, 138, 11810–11819

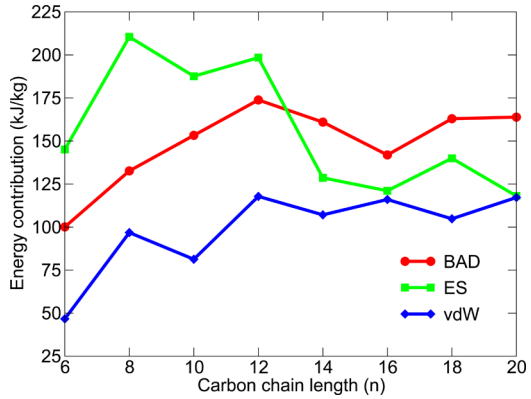

Figure 6. Changes of the contributions of bonded (BAD, red), electrostatic (ES, green), and van der Waals (vdW, blue) energies to thermal storage density along the carbon chain length. Unit in kJ/kg.

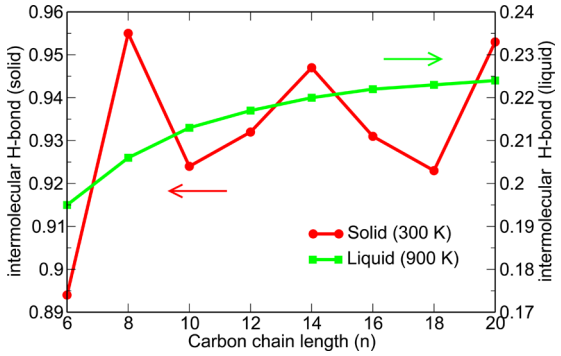

Figure 7. Number of intermolecular H-bonds per OH group obtained by the solid phase simulations at 300 K (red, left axis) and by the liquid simulations at 900 K (green, right axis).

qualitatively consistent with that of the previous study of the six-carbon sugar alcohols.[16]

Effect of Carbon Chain Elongation on the ES Contribution. We then analyzed the carbon chain elongation effect on each contribution. The ES contribution is first considered. Figure 6 shows that the ES contribution seems to be affected by several factors because it does not necessarily increase with the carbon chain length. We found that two factors are related mainly to this behavior of the ES contribution: the melting points and the ES stability in the solid phase. It was demonstrated by MD simulations that the high temperature leads to the large difference of ES energy between the solid and liquid phases (Figure S5a). This indicates that a sugar alcohol with a higher melting point provides the larger ES contribution to thermal storage density. Since the rising melting point originates from the carbon chain elongation as shown above (Figure 3), the ES contribution is indirectly affected by the carbon chain length through melting points. The results that the ES contribution of the **C6** sugar alcohol is especially small compared to others and the **C10** sugar alcohol has smaller ES contribution than the **C12** sugar alcohol are attributed to their lower melting points.

However, the largest ES contribution of the **C8** sugar alcohol cannot be interpreted by the melting point effect because its melting point is comparable to the **C10** sugar alcohol's one and is much lower than the **C12** sugar alcohol's one. Since the ES energy in sugar alcohols is greatly influenced by intermolecular H-bonds, we investigated the relationship between the H-bonds and the carbon chain length in order to find a clue to the understanding of the largest ES contribution of the **C8** sugar alcohol. Figure 7 plots the number of intermolecular H-bonds per OH group in the solid (300 K) and liquid (900 K) phases separately along the carbon chain length.[35,36] Performing this analysis at the given temperatures allows us to exclude the melting point effect. It should be noted that although the absolute values of that number of H-bonds depend on the given temperatures, the relative ones among the **C6**−**C12** sugar alcohols are almost not affected by the temperatures. Also, each **C6**−**C12** sugar alcohol can be in stable solid and liquid phases at those temperatures. From this figure, we found that the number of H-bonds in the liquid phase monotonically increases with the carbon chain length. However, the changes of the number of H-bonds in the liquid phase are smaller than those in the solid phase, which implies that the ES contribution is largely affected by the solid phase rather than by the liquid phase. In addition, more importantly, those changes in the solid phase do not correlate with the carbon chain length. This indicates that the difference of the number of intermolecular H-bonds between the solid and liquid phases does not necessarily increase with the carbon chain length. Looking at the largest ES contribution of the **C8** sugar alcohol with these H-bond changes in mind, we found that its slightly larger number of intermolecular H-bonds in the solid phase (compared to those H-bonds of the **C10** and **C12** sugar alcohols) seems to cause the largest ES contribution. That is, the **C8** sugar alcohol has the irregularly stable solid phase in terms of ES energy, compared to the other sugar alcohols. Actually, the irregularly low ES energy in the solid phase of the **C8** sugar alcohol was observed (Figure S6). From these results, it was suggested that the ES contribution excluding the melting point effect depends largely, not on the carbon chain length, but on the ES stability in the solid phase of each sugar alcohol.

Effect of Carbon Chain Elongation on the BAD Contribution. In contrast to the ES contribution, the BAD contribution among the **C6**−**C12** sugar alcohols was found to increase with the carbon chain length (Figure 6). To elucidate the mechanism, we considered the BAD energies of the solid (300 K) and liquid (900 K) phases separately at the given temperatures as with the intermolecular H-bond analysis above. It should be noted that the result shown below is almost unchanged even if the other temperatures were selected for this analysis. The relative BAD energies of the **C8**−**C12** sugar alcohols with respect to the **C6** sugar alcohol $\Delta E_{BAD}^{phase}(n)$ (= $E_{BAD}^{phase}(n) - E_{BAD}^{phase}(6)$, n stands for the carbon chain length) are depicted for both phases in Figure 8.[37] Compared to the relative BAD energy in the solid phase $\Delta E_{BAD}^{solid}(n)$ (red curve in Figure 8), that in the liquid phase $\Delta E_{BAD}^{liquid}(n)$ (green curve in Figure 8) greatly changes with the carbon chain length. This indicates that the dependence of the BAD contribution on the carbon chain length stems from the BAD energy in the liquid phase. Since the increase in $\Delta E_{BAD}^{liquid}(n)$ is favorable to the large BAD contribution, this result is consistent with the increase in the BAD contribution shown in Figure 6. Therefore, we concluded that the BAD contribution is enhanced by the direct effect of the carbon chain elongation regardless of the melting points.

In order to elucidate the mechanism of the increase in $\Delta E_{BAD}^{liquid}(n)$, we divided a linear structure of sugar alcohol into three parts, i.e., two terminal regions and one middle region, and analyzed their contributions to $\Delta E_{BAD}^{liquid}(n)$ qualitatively. The terminal regions are defined as the two CH_2OH−CHOH

DOI: 10.1021/jacs.6b05902
J. Am. Chem. Soc. 2016, 138, 11810−11819

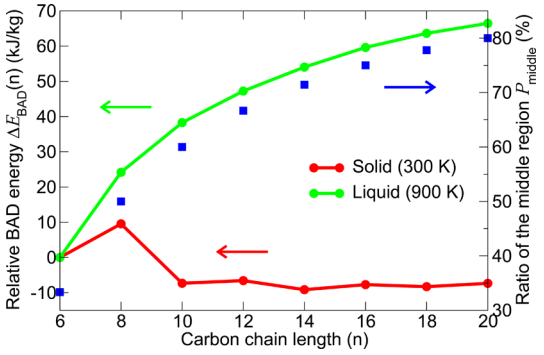

Figure 8. Relative BAD energy with respect to the BAD energy of the **C6** sugar alcohol, i.e., $\Delta E_{BAD}(n) = E_{BAD}(n) - E_{BAD}(6)$, along the carbon chain length: red and green curves were obtained from MD simulations at 300 K (solid) and 900 K (liquid), respectively. Additionally, the ratio of the number of CHOH units in the middle region to the total number of CHOH and CH_2OH units in a molecule, P_{middle}, is also plotted by blue squares along the carbon chain length. See the main text for the definition of the middle region.

segments at each end of a molecule, and the middle region is defined as the remaining part between them (see Figure S7). It is clear that the linear carbon chain elongation increases the ratio of the number of CHOH units in the middle region to the total number of CHOH and CH_2OH units in a molecule (denoted by P_{middle}, see Figure 8). Around an OH group in the middle region, there are more OH groups to act as an intramolecular H-bond donor or acceptor, compared to an OH group in the terminal regions. Consequently, in the liquid phase, more intramolecular H-bonds are formed in the middle region than in the terminal region (Figure S8). The formation of such intramolecular H-bonds causes the distorting molecular structure, thus it leads to the increase in the BAD energy.[38] In this way, we can naturally come to the conclusion that the carbon chain elongation directly causes the increase in $\Delta E_{BAD}^{liquid}(n)$ shown in Figure 8. In addition to the monotonic increase behavior, we obviously found that a gradual decrease in the increment of $\Delta E_{BAD}^{liquid}(n)$ with the carbon chain length is also attributed to the ratio P_{middle}. Therefore, the changes of the BAD contribution are well explained by clarifying the difference between the terminal and middle regions in a carbon backbone. This strategy for the interpretation may be related to the well-known idea in a polymer system that regions near end groups in a polymer act as potential impurities or defects.[39,40]

Effect of Carbon Chain Elongation on the vdW Contribution. The vdW contribution is also shown in Figure 6. This contribution increases with oscillation, not monotonically, as the carbon chain becomes longer. This oscillation is correlated very well with molecular mass density of the crystal (Figure S9a), which is likely to originate from the difference of molecular symmetry between chiral (**C6** and **C10**) and achiral (**C8** and **C12**) sugar alcohols. In addition, we found that the increase behavior of the vdW contribution comes from the effect of the rising melting points as the ES contribution does (see Figure S5c and S9b).

*Thermal Storage Densities of the **C14−C20** Sugar Alcohols.* At the end of this section, we consider thermal storage density of the **C14−C20** sugar alcohols. As mentioned above, the **C14−C20** sugar alcohols melt through their premelting phases with broken intermolecular H-bond networks in the carbon-chain end groups. The result that the ES contribution decreases significantly compared to that of the **C12** sugar alcohol (green plot in Figure 6) is clearly due to the partly broken H-bond networks. The BAD contribution also decreases in the **C14−C20** sugar alcohols relative to the **C12** sugar alcohol (red plot in Figure 6). This is also attributed to the liquid-like disordered end groups of a carbon backbone in the premelting phase. Furthermore, this disordering in the end groups increases in some degree the system volume (Figure S10), resulting in the decrease in molecular mass density of the solid. This decrease leads to the unstable solid phase in terms of vdW energy. Thus, in spite of the high melting points of the **C14−C20** sugar alcohols, their vdW contributions are comparable to that of the **C12** sugar alcohol.

3.6. Thermal Storage Densities of C8 Isomers: Effect of OH Group Distribution. In the previous study,[16] we proposed preferable isomers for large thermal storage density. The proposition argues that such isomers must locate OH groups separately as far as possible in order to avoid unstable molecular structures in the crystal. To confirm this proposition, we considered other two isomers of the **C8** sugar alcohol employed above. They are shown in Figure 9. One is a

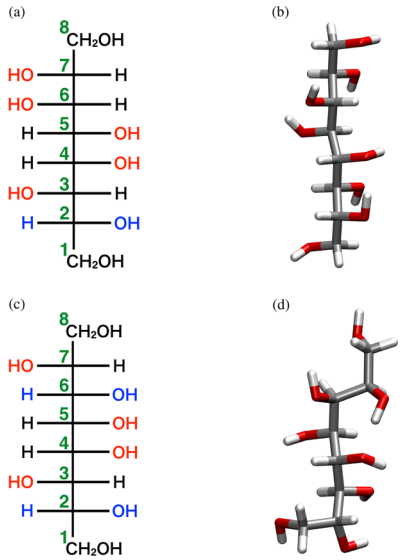

Figure 9. Chemical formulas and molecular structures in the crystal of two eight-carbon non-natural sugar alcohol isomers. (a) and (b): **C8I** sugar alcohol, the OH group and the hydrogen atom at the C2-position are replaced each other with respect to the **C8** sugar alcohol. (c) and (d): **C8II** sugar alcohol, the OH group and the hydrogen atom at the C6-position are further replaced each other with respect to the former. The index of carbon atoms is represented by green numbers. The atoms and groups altered from the **C8** sugar alcohol are represented by blue colors.

molecule formed from the **C8** sugar alcohol by replacing the OH group with the hydrogen atom in the C2-position (Figure 9a). The other molecule is formed from the former by further replacing the OH group with the hydrogen atom in the C6-position (Figure 9c). In this paper, we will call the former and latter molecules **C8I** and **C8II** sugar alcohols, respectively. These exchanges between an OH group and a hydrogen atom give the 1−3 parallel interaction in their extended conformations: the **C8I** sugar alcohol has a parallel orientation between the C2−O and C4−O bonds, and the **C8II** sugar alcohol has another additional one between the C6−O and C4−O bonds.

Next, we predicted crystal structures of the **C8I** and **C8II** sugar alcohols. The molecular structures in their predicted

DOI: 10.1021/jacs.6b05902
J. Am. Chem. Soc. 2016, 138, 11810−11819

crystal structure are also shown in Figure 9. It is well-known that molecules with the 1−3 parallel interaction in the extended conformation are likely to form a bending molecular structure in the crystal,[27] but we found that the **C8I** sugar alcohol has the extended conformation despite the 1−3 parallel interaction between the C2−O and C4−O bonds. A closer look at these bonds revealed the intramolecular H-bond between these OH groups. The distance between the hydrogen and the acceptor oxygen atoms ($R(H-O_a)$) was 1.895 Å and the angle O−H···O ($\angle O_dHO_a$) was 143.8° at the first-principles level, which are obviously classified as an H-bond. On the other hand, the **C8II** sugar alcohol in the crystal bends at two positions of the C2 and C6 atoms. This bending conformation is a result from the avoidance of two 1−3 parallel interactions. Another feature of this structure is an intramolecular H-bond between the OH groups connected to the C4 and C7 atoms, where $R(H-O_a)$ = 1.720 Å and $\angle O_dHO_a$ = 162.3° at the first-principles level. It should be noted that in compensation for these intramolecular H-bonds some intermolecular H-bonds are lost in those crystals (Table S6). In the case of sugar alcohols, it is rare to find intramolecular H-bonds in the crystal, but they are not unknown at all. Such H-bonds are indeed observed experimentally in the artificially synthesized ten-carbon sugar alcohol.[41]

With the predicted crystal structures we evaluated melting points and thermal storage densities of the **C8I** and **C8II** sugar alcohols. The results are listed in Table 1. We found that the

Table 1. Melting Points (K) and Thermal Storage Densities (kJ/kg) of the Eight-Carbon Non-natural Sugar Alcohols

sugar alcohol	melting point	thermal storage density
C8	600	440
C8I	480	257
C8II	400[a]	136

[a]The corresponding experimental value is 395 K.[42]

C8I sugar alcohol has the lower melting point (480 K) and the smaller thermal storage density (~260 kJ/kg) compared to the original **C8** sugar alcohol. For the **C8II** sugar alcohol, compared to the **C8I** sugar alcohol, the further decreases in melting point and thermal storage density to 400 K and ~135 kJ/kg were observed, respectively. (Fortunately, we were able to find the experimental melting point of the **C8II** sugar alcohol, which was about 395 K.[42]) From the decomposition analysis, it was found that these decreases in thermal storage density originate directly from the significantly unstable solid phases (see Table S7). These unstable solid phases are attributed to the destabilized ES energy which is caused by the loss of intermolecular H-bonds. In addition, the solid phase of the **C8II** sugar alcohol is also quite unstable in terms of vdW energy (Table S7). This may be related to its complicated bending molecular structure in the crystal which is unlikely to form the dense crystal packing.

4. DISCUSSION

As mentioned in Introduction, high performance PCMs with large thermal storage density are highly demanded for the effective reuse of waste heat. Yet the limit of existing organic PCMs is still ~350 kJ/kg of thermal storage density provided by natural sugar alcohols. It has been unclear how large thermal storage density can be achieved by organic PCMs potentially, and the question has hardly been investigated as long as we know. In this study we answered the issue, in the sugar alcohol case as an example of polar organics, using the computational approach. We found that it is in principle possible to achieve remarkably large thermal storage density (~450−500 kJ/kg), which goes beyond the limit of existing organic PCMs, by modeling sugar-alcohol-like molecules in accordance with our molecular design guidelines. This insight gives us great hope and possibility of finding new high performance PCMs in both experimental and computational researches.

The remarkably large thermal storage density in this study was achieved by the carbon chain elongation and selection of preferable isomers of sugar alcohol molecules. From the analysis of the carbon chain elongation effect, it was suggested that the BAD and vdW contributions also play an important role in increase in thermal storage density even in the case of H-bonded molecular crystals where the ES energy contributes mainly to thermal storage density. In particular, the BAD contribution directly increases thermal storage density by the elongation regardless of the melting points. Although the resultant elongation effect was different from the original intent (see Introduction and ref 16), the elongation was certainly shown to make a critical impact on thermal storage density. However, it was also indicated that the excessive carbon chain elongation is unfavorable to large thermal storage density due to the occurrence of the solid−solid phase transition observed in the much longer molecules such as the **C14−C20** sugar alcohols. As well as the carbon chain elongation, the distribution of OH groups was confirmed to be a critical viewpoint for achieving large thermal storage density through the comparison between the eight-carbon sugar alcohol isomers. However, it should be noted that the guideline is still not completely accepted because we investigated no more than two molecules among a large number of isomers. Nevertheless, the result that the **C8I** and **C8II** sugar alcohols have much smaller thermal storage densities than the **C8** sugar alcohol suggests the deep relationship between thermal storage density and molecular structures of isomers. Therefore, in order to achieve large thermal storage density, the guidelines employed in this study, in particular linear elongation of a carbon backbone and separated distribution of OH groups, can be valuable suggestions for sugar-alcohol-like PCMs.

In addition, we clearly demonstrated, through the thermal storage density calculations of the non-natural sugar alcohols, that the computational approach is a powerful way to predict the concerned thermophysical properties of experimentally unknown PCMs. The present calculations were performed by conventional computational methods, so that they are not specific to sugar alcohol series. Therefore, the computational approach can be effectively utilized not only to propose some molecular design guidelines for new PCMs but also to validate the propositions and screen candidate materials. We believe that this powerful approach comparable to experimental one further accelerates the development of high performance PCMs.

Finally, we briefly remark on the melting points of the non-natural sugar alcohols as PCMs. Although the thermal storage densities of the non-natural sugar alcohols were successfully increased, their melting points were not optimized for practical usage. Indeed, the melting points of the **C12−C20** sugar alcohols (>700 K) may be too high for their usage as PCMs because of a risk of molecular degradation. In the viewpoint of practical applications of PCMs, melting point (i.e., temperature of operation) must be one of the important factors. Therefore,

DOI: 10.1021/jacs.6b05902
J. Am. Chem. Soc. 2016, 138, 11810−11819

future work should pay attention to this issue as well as the main subject of the increase in thermal storage density.

Nevertheless, it is also true that organic PCMs which work at high temperature have advantages in thermal management applications. It is well-known that there is a huge amount of waste heat whose temperature is in the range between 400 and 600 K (~100−300 °C) in various systems, such as automobile engines and industrial plants. At present, we have no organic PCMs which can handle such high temperature heat. If we prepare the non-natural sugar alcohols with the relatively high melting point (~600 K), we will be able to reutilize these waste heat by using PCM technology. We expect that such organic PCMs with high melting points and large thermal storage densities will extend the range of thermal management applications in the various social systems and stimulate the development of the waste heat recovery systems for high temperature applications.

5. CONCLUSIONS

In this study, we computationally predicted thermal storage density of the non-natural sugar alcohols as a basic step toward the development of new PCMs with large thermal storage density. These sugar alcohols were constructed in silico in accordance with the three molecular design guidelines: linear elongation of a carbon backbone, separated distribution of OH groups, and even numbers of carbon atoms, and their crystal structures were predicted by the random search method and first-principles calculations. As a result, it was demonstrated that thus constructed non-natural sugar alcohols have potential ability to have thermal storage density up to ~450−500 kJ/kg, which is significantly larger than the maximum thermal storage density of the present known organic PCMs (~350 kJ/kg). It was found that the BAD contribution was a key factor to directly increase thermal storage density by the carbon chain elongation regardless of the melting points. For the ES and vdW contribution, the elongation indirectly increases thermal storage density through the rising melting point. These results suggest that even in the case of H-bonded molecular crystals like sugar alcohols, where the ES energy contributes mainly to thermal storage density, the other molecular distortion (i.e., BAD) and vdW energies are also important factors to increase thermal storage density. Furthermore, the comparison between the three eight-carbon sugar alcohol isomers indicated that the selection of preferable isomers is also essential for large thermal storage density. Overall, the present computational study suggests that it is in principle possible to achieve large thermal storage density that goes beyond the limit of existing organic PCMs by properly designing sugar-alcohol-like molecules.

■ ASSOCIATED CONTENT

Supporting Information

The Supporting Information is available free of charge on the ACS Publications website at DOI: 10.1021/jacs.6b05902.

Computational details for crystal structure predictions; computational details for thermal storage density; detailed results of crystal structure predictions; and supplementary tables and figures noted in the main text (PDF)

Crystal structures (CIF) used to calculate thermal storage density (ZIP)

■ AUTHOR INFORMATION

Corresponding Authors

*inagaki@ncube.human.nagoya-u.ac.jp

*toyokazu.ishida@aist.go.jp

Present Address

#Graduate School of Information Science, Nagoya University, Furo-cho, Chikusa-ku, Nagoya 464-8601, Japan.

Notes

The authors declare no competing financial interest.

■ ACKNOWLEDGMENTS

This work was supported by New Energy and Industrial Technology Development Organization (NEDO), and Future Pioneering Projects of Ministry of Economy, Trade and Industry (METI), Japan. Molecular and crystal figures are created with VMD[43] and Mercury.[44]

■ REFERENCES

(1) Yan, T.; Wang, R.; Li, T.; Wang, L.; Fred, I. T. *Renewable Sustainable Energy Rev.* **2015**, *43*, 13−31.

(2) Arteconi, A.; Hewitt, N.; Polonara, F. *Appl. Energy* **2012**, *93*, 371−389.

(3) Tian, Y.; Zhao, C. *Appl. Energy* **2013**, *104*, 538−553.

(4) Sharma, S.; Sagara, K. *Int. J. Green Energy* **2005**, *2*, 1−56.

(5) Nomura, T.; Okinaka, N.; Akiyama, T. *ISIJ Int.* **2010**, *50*, 1229−1239.

(6) Kenisarin, M. M. *Sol. Energy* **2014**, *107*, 553−575.

(7) Tokoro, H.; Yoshikiyo, M.; Imoto, K.; Namai, A.; Nasu, T.; Nakagawa, K.; Ozaki, N.; Hakoe, F.; Tanaka, K.; Chiba, K.; Makiura, R.; Prassides, K.; ichi Ohkoshi, S. *Nat. Commun.* **2015**, *6*, 7037.

(8) Cabeza, L.; Mehling, H.; Hiebler, S.; Ziegler, F. *Appl. Therm. Eng.* **2002**, *22*, 1141−1151.

(9) Sharma, A.; Tyagi, V. V.; Chen, C. R.; Buddhi, D. *Renewable Sustainable Energy Rev.* **2009**, *13*, 318−345.

(10) Sole, A.; Neumann, H.; Niedermaier, S.; Martorell, I.; Schossig, P.; Cabeza, L. F. *Sol. Energy Mater. Sol. Cells* **2014**, *126*, 125−134.

(11) Kenisarin, M.; Mahkamov, K. *Renewable Sustainable Energy Rev.* **2007**, *11*, 1913−1965.

(12) Grembecka, M. *Eur. Food Res. Technol.* **2015**, *241*, 1−14.

(13) Prajapati, B. G.; Ratnakar, N. *Int. J. PharmTech Res.* **2009**, *1*, 790−798.

(14) Nakano, K.; Masuda, Y.; Daiguji, H. *J. Phys. Chem. C* **2015**, *119*, 4769−4777.

(15) Oya, T.; Nomura, T.; Tsubota, M.; Okinaka, N.; Akiyama, T. *Appl. Therm. Eng.* **2013**, *61*, 825−828.

(16) Inagaki, T.; Ishida, T. *J. Phys. Chem. C* **2016**, *120*, 7903−7915.

(17) Jain, A.; Shin, Y.; Persson, K. A. *Nat. Rev. Mater.* **2016**, *1*, 15004.

(18) Curtarolo, S.; Hart, G. L. W.; Nardelli, M. B.; Mingo, N.; Sanvito, S.; Levy, O. *Nat. Mater.* **2013**, *12*, 191−201.

(19) van Eijck, B. P.; Kroon, J. *Acta Crystallogr., Sect. B: Struct. Sci.* **2000**, *56*, 535−542.

(20) Giannozzi, P.; Baroni, S.; Bonini, N.; Calandra, M.; Car, R.; Cavazzoni, C.; Ceresoli, D.; Chiarotti, G. L.; Cococcioni, M.; Dabo, I.; Dal Corso, A.; de Gironcoli, S.; Fabris, S.; Fratesi, G.; Gebauer, R.; Gerstmann, U.; Gougoussis, C.; Kokalj, A.; Lazzeri, M.; Martin-Samos, L.; Marzari, N.; Mauri, F.; Mazzarello, R.; Paolini, S.; Pasquarello, A.; Paulatto, L.; Sbraccia, C.; Scandolo, S.; Sclauzero, G.; Seitsonen, A. P.; Smogunov, A.; Umari, P.; Wentzcovitch, R. M. *J. Phys.: Condens. Matter* **2009**, *21*, 395502.

(21) Belonoshko, A. B.; Ahuja, R.; Johansson, B. *Phys. Rev. Lett.* **2000**, *84*, 3638−3641.

(22) Cornell, W. D.; Cieplak, P.; Bayly, C. I.; Gould, I. R.; Merz, K. M.; Ferguson, D. M.; Spellmeyer, D. C.; Fox, T.; Caldwell, J. W.; Kollman, P. A. *J. Am. Chem. Soc.* **1995**, *117*, 5179−5197.

(23) Damm, W.; Frontera, A.; Tirado-Rives, J.; Jorgensen, W. L. *J. Comput. Chem.* **1997**, *18*, 1955−1970.

(24) Pronk, S.; Pall, S.; Schulz, R.; Larsson, P.; Bjelkmar, P.; Apostolov, R.; Shirts, M. R.; Smith, J. C.; Kasson, P. M.; van der Spoel, D.; Hess, B.; Lindahl, E. *Bioinformatics* **2013**, *29*, 845−854.
(25) Bardwell, D. A.; Adjiman, C. S.; Arnautova, Y. A.; Bartashevich, E.; Boerrigter, S. X. M.; Braun, D. E.; Cruz-Cabeza, A. J.; Day, G. M.; Della Valle, R. G.; Desiraju, G. R.; van Eijck, B. P.; Facelli, J. C.; Ferraro, M. B.; Grillo, D.; Habgood, M.; Hofmann, D. W. M.; Hofmann, F.; Jose, K. V. J.; Karamertzanis, P. G.; Kazantsev, A. V.; Kendrick, J.; Kuleshova, L. N.; Leusen, F. J. J.; Maleev, A. V.; Misquitta, A. J.; Mohamed, S.; Needs, R. J.; Neumann, M. A.; Nikylov, D.; Orendt, A. M.; Pal, R.; Pantelides, C. C.; Pickard, C. J.; Price, L. S.; Price, S. L.; Scheraga, H. A.; van de Streek, J.; Thakur, T. S.; Tiwari, S.; Venuti, E.; Zhitkov, I. K. *Acta Crystallogr., Sect. B: Struct. Sci.* **2011**, *67*, 535−551.
(26) Neumann, M.; Leusen, F.; Kendrick, J. *Angew. Chem., Int. Ed.* **2008**, *47*, 2427−2430.
(27) Kim, S. H.; Jeffrey, G. A. *Carbohydr. Res.* **1970**, *14*, 207−216.
(28) According to the molecular design guidelines, we are also able to construct molecular formulae that can be regarded as the extension of galactitol, one of the six-carbon natural sugar alcohols. But, we constructed mannitol-based molecules because mannitol is more famous in various fields and more accessible in experiments than galactitol
(29) Laasonen, K.; Parrinello, M.; Car, R.; Lee, C.; Vanderbilt, D. *Chem. Phys. Lett.* **1993**, *207*, 208−213.
(30) Matsumoto, M.; Saito, S.; Ohmine, I. *Nature* **2002**, *416*, 409−413.
(31) Berman, H. M.; Jeffrey, G. A.; Rosenstein, R. D. *Acta Crystallogr., Sect. B: Struct. Crystallogr. Cryst. Chem.* **1968**, *24*, 442−449.
(32) Barone, G.; Gatta, G. D.; Ferro, D.; Piacente, V. *J. Chem. Soc., Faraday Trans.* **1990**, *86*, 75.
(33) Maroncelli, M.; Qi, S. P.; Strauss, H. L.; Snyder, R. G. *J. Am. Chem. Soc.* **1982**, *104*, 6237−6247.
(34) Thermal storage density is evaluated from the enthalpy difference between the solid and liquid phases. The pressure−volume product term contributes only negligibly to the difference at normal pressure, and the kinetic energy difference between the two phases does not contribute to that at a given temperature (e.g., melting point).
(35) An H-bond where the distance between a donor oxygen O_D and an acceptor oxygen O_A atoms is less than 3.0 Å and the angle O_D−H···O_A is larger than 100° was counted.
(36) This figure also includes the numbers of H-bonds for the **C14**−**C20** sugar alcohols in order to properly capture the whole trend of those H-bonds. It should be noted that those numbers at 300 and 900 K are not affected by the premelting phases of the **C14**−**C20** sugar alcohols.
(37) For the same reason as in Figure 7, this figure also includes the BAD energies for the **C14**−**C20** sugar alcohols.
(38) Influence of intramolecular H-bonds formed in this way on thermal storage density is naturally included in the ES contribution.
(39) Fox, T. G.; Flory, P. J. *J. Appl. Phys.* **1950**, *21*, 581−591.
(40) Hale, A.; Macosko, C. W.; Bair, H. E. *Macromolecules* **1991**, *24*, 2610−2621.
(41) Köll, P.; Kopf, J.; Morf, M.; Zimmer, B.; Brimacombe, J. S. *Carbohydr. Res.* **1992**, *237*, 289−293.
(42) Brimacombe, J. S.; Kabir, A. K. *Carbohydr. Res.* **1987**, *168*, C5−C7.
(43) Humphrey, W.; Dalke, A.; Schulten, K. *J. Mol. Graphics* **1996**, *14*, 33−38.
(44) Macrae, C. F.; Bruno, I. J.; Chisholm, J. A.; Edgington, P. R.; McCabe, P.; Pidcock, E.; Rodriguez-Monge, L.; Taylor, R.; van de Streek, J.; Wood, P. A. *J. Appl. Crystallogr.* **2008**, *41*, 466−470.

DOI: 10.1021/jacs.6b05902
J. Am. Chem. Soc. 2016, 138, 11810−11819